11th International Tribology Conference
SAIT TRIBOLOGY 2015
10-12 March 2015, Pretoria, South Africa
Paper ID: SAIT2015-xxx

ASPERITY CONTACT MODELLING FOR MEASURED SURFACES

Leighton M, Morris N, Rahmani R, Rahnejat H

Loughborough University, Loughborough, UK

ABSTRACT

The analysis of surface roughness in contacts forms a major part of tribology in almost all application. In any contact in which asperity interactions occur their load carrying capacity must be considered however the separation at which asperity interaction first occurs and the load carrying capacity at that separation are due to the stochastic nature of the surface roughness of the two surfaces. A model that can accurately and quickly provide an estimation of the load carrying capacity as a function of surface separation is required for the specific surfaces used in such conjunctions from implementing surface data.

The paper presented provides details of a procedure for modeling asperity interactions of rough surfaces from measured data. The model is validated against a deterministic approach before being applied to measured surfaces.

Keywords: Load, Roughness, Friction, Piston Ring, Cylinder Liner

NONMENCLATURE

Symbols

$\mathcal{A}$	Apparent Area of contact
β	Asperity tip radius of curvature
d	Separation between surface mean centerlines
η	Asperity density
E'	Composite Elastic Modulus
$\mathrm{F}_{\frac{5}{2}}$	Statistical function
λ	Stribeck Parameter
P	Load
$\tilde{P}$	Mean load
ϕ	Probability distribution function
ϕ^*	Convoluted probability distribution function
r	Radial distance between asperity tips
w_p	Vertical interference between asperity tips
z	Surface height

1. INTRODUCTION

Historically there have been two major components to the modelling of load carrying capacity for sliding rough surfaces in a lubricated contact; an analysis of asperity interactions and lubricant pressure (Mishra, 2008) (Morris, 2013) (Rahmani, 2012). Sliding rough surfaces with a lubricating film come into almost all engineering applications although the most common applications; bearings, gears and engine power-train components, strive for continued advancement in performance through improved modelling. A balance of the load carried between these two mechanisms is general generally sort with load carrying capacity contributions from both increasing as the surfaces move together but at different non-linear rates.

An improved understanding of the asperity interactions and how they are modelled is sort for specific measured surface geometry. The analysis of the specific surfaces used in a given application can provide significant improvements in the accuracy of the modelling although the extension to measured data for some theories can prove problematic.

Greenwood and Tripp (Greenwood, 1971) provided a continuation of the work of Greenwood and Williamson (Greenwood, 1966), which mathematically modelled the asperity interactions between rough surfaces, by considering the surface probability distributions and mechanical interactions of simplified asperity geometry. Greenwood and Tripp made a series of assumptions to simplify the conditions of the contact, the most crucial of these was that the asperities can be modelled as a collection of spheres of the same radius as the average tip radius of the surfaces and all indenting a similar sphere on the counter surface by the same amount, the average indentation depth of the asperities at a certain separation, while accounting for the possibility of the asperities contacting when misaligned. This is a necessarily complex set of assumptions which are determined through a tougher consideration of the nature of rough surface interactions.

2. METHOD

Beginning with the assumption that the surfaces have been replaced by collections of spheres of the same radius, β, (**Figure 1**) as the average tip radius of curvature calculated from both surface and the same peak height distribution as the original surfaces the surface interaction can be described mathematically.

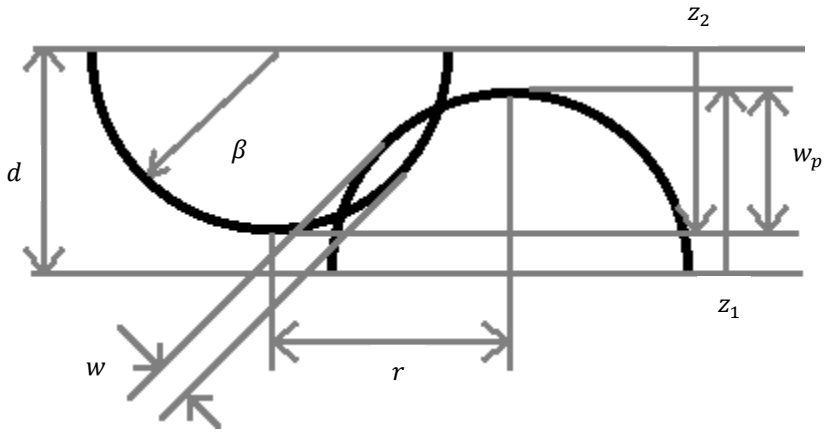

Figure 1 Asperity interaction diagram

The average asperity density over both surfaces is η and the area being considered is $\mathcal{A}$. Therefore the probable load supported by this representative surface at a given separation, $\tilde{P}(d)$, can be shown to be,

$$\tilde{P}(d) = 2\pi\eta^2\mathcal{A}\int_r\int_{z_1}\int_{z_2} P(w,r)\phi(z_1)\phi(z_2)r.\,dz_2.\,dz_1.\,dr \tag{1}$$

This states that the probable load is the product of the load supported at a given interference between one pair of asperities, the probability of an asperity on one surface at that position and the probability of an asperity on the remaining surface at that position for all possible radial positions and possible surface heights and multiplied by the total number of possible contacts.

Examples of measured surface frequency distributions can be seen in the work of Peklenik (Peklenik, 1967) which also discusses some of the key variations between measured and generated surface properties.

Combining the probabilities by taking the convolution of the asperity peak height distributions for each surface,

$$\phi^*(z) = \phi(z_1) * \phi(z_2) \tag{2}$$

And using the Hertzian theory to express the load carrying capacity as a function of the interference of two spheres of the same radius, β, and composite elastic modulus, E', by,

$$P = \frac{4}{3}E'\left(\frac{\beta}{2}\right)^{\frac{1}{2}}w^{\frac{3}{2}} \tag{3}$$

Equation (1) reduces to,

$$\tilde{P}(d) = 2\pi\eta^2\mathcal{A}\int_r\int_z\left(\frac{4}{3}\right)E'\left(\frac{\beta}{2}\right)^{\frac{1}{2}}w^{\frac{3}{2}}\phi^*(z)r.\,dz.\,dr \tag{4}$$

Assuming that the angle to the vertical at which contact occurs, after two misaligned asperities contact, is negligible then w can be simply expressed as a function of w_p and r given that the asperity shape is spherical.

$$w = \langle w_p - \frac{r^2}{4\beta}\rangle \tag{5}$$

Where $\langle\ \rangle$ is a Macauley bracket. The equation for probable load at a given separation therefore simplifies further to,

$$\tilde{P}(d) = 2\pi\eta^2\mathcal{A}\int_r\int_z\left(\frac{4}{3}\right)E'\left(\frac{\beta}{2}\right)^{\frac{1}{2}}\langle w_p - \frac{r^2}{4\beta}\rangle^{\frac{3}{2}}\phi^*(z)r.\,dz.\,dr \tag{6}$$

Extracting constants and setting the limits of the integrations,

$$\tilde{P}(d) = \frac{8}{3}\pi\eta^2E'\left(\frac{\beta}{2}\right)^{\frac{1}{2}}\mathcal{A}\int_d^\infty\phi^*(z).\,dz\int_0^\infty\langle w_p - \frac{r^2}{4\beta}\rangle^{\frac{3}{2}}r.\,dr \tag{7}$$

$$\tilde{P}(d) = \frac{8}{3}\pi\eta^2E'\left(\frac{\beta}{2}\right)^{\frac{1}{2}}\mathcal{A}\int_d^\infty\phi^*(z).\,dz\left[-\frac{4}{5}\beta\langle w_p - \frac{r^2}{4\beta}\rangle^{\frac{5}{2}}\right]_0^\infty \tag{8}$$

$$\tilde{P}(d) = \frac{16\sqrt{2}}{15}\pi\eta^2\beta^{\frac{3}{2}}E'\mathcal{A}\int_d^\infty\langle z-d\rangle^{\frac{5}{2}}\phi^*(z).\,dz \tag{9}$$

Standardising the form of the probability distribution by taking the distribution in terms of $s = \sigma z$

$$\tilde{P}(d) = \frac{16\sqrt{2}}{15}\pi\eta^2\beta^{\frac{3}{2}}\sigma^{\frac{5}{2}}E'\mathcal{A}\int_{\frac{d}{\sigma}}^\infty\left(s-\frac{d}{\sigma}\right)^{\frac{5}{2}}\phi^*(s).\,ds \tag{10}$$

Equation (10) then rearranges into the form given by Greenwood and Tripp,

$$\tilde{P}(d) = \frac{16\sqrt{2}}{15}\pi(\eta\beta\sigma)^2E'\sqrt{\frac{\sigma}{\beta}}\mathcal{A}\mathrm{F}_{\frac{5}{2}}\left(\frac{d}{\sigma}\right) \tag{11}$$

Where,

$$F_{\frac{5}{2}}(\lambda) = \int_\lambda^\infty(s-\lambda)^{\frac{5}{2}}\phi^*(s).\,ds \tag{12}$$

The function, $F_{\frac{5}{2}}(\lambda)$, represents the statistical likelihood of interactions and the distance the asperities are compressed by for all the possible position of one surface lowered onto another as the surfaces are being analysed for sliding contacts. This function, together with η, β and σ, represent the roughness specific input for the model Greenwood and Tripp proposed. In order to maximise the accuracy of this model for a specific set of surfaces these roughness specific parameters must be calculated. η, β and σ can be simply calculated with many commercially available metrology softwares however $F_{\frac{5}{2}}(\lambda)$ can have a significant contribution to the accuracy of the model and is more complicated to determine from surface data.

3. EXTENSION TO MEASURED SURFACE DATA

Measuring the topography of a surface with most modern measurement machines provides an array of data giving the surface height at discrete measured nodes. This is essential for any further manipulation of that data for models such as this but does convert the continuous surface height data into discrete data at the nodes of the array. The surface data can be used in probabilistic models, such as this; however the frequency distributions required will be a discrete step histogram for each surface.

Identifying the asperity points and their heights allows a discrete peak height distribution for each surface to be determined. The convolution of the two peak height distributions can then be found. This convolution function, ϕ^*, must be adjusted such that,

$$\int_{-\infty}^{\infty} \phi^*(x).dx = 1 \tag{13}$$

So that the total probability equals unity and the standard deviation set to σ, the combined RMS of the surface heights. It is then a simple calculation to find $F_{\frac{5}{2}}(\lambda)$ for any desired surface height through an integration of the histogram columns above the λ value being considered with a weighting as shown in equation (12).

4. VALIDATION

A program to calculate the function $F_{\frac{5}{2}}(\lambda)$ for a given surface input was validated against a deterministic model which provided no contradictions to the assumptions outlined in Greenwood and Tripp. Consider two surfaces which each consist of a single, hemi-spherical asperity; at a given separation their two tips may overlap each other by a distance w_p. This results in a compressive distance, w, as described in equation (5) and shown in **Figure 1**. If the integral of r from 0 to ∞ were taken deterministically it would be necessary to calculate the load carrying capacity of the surface interactions at each possible nodal position for a given separation and introduce a probabilistic likelihood by dividing by the total possible positions. The magnitude of r can be determined for such a simple surface as there is only one asperity on each surface and their relative positions are known. The load carried at each position, P, must be calculated by equation (3) and w by equation (5) so that the assumptions of the Greenwood and Tripp model are extended. Using this approach it is possible to determine the load carrying capacity as a function of surface separation.

A comparison of the deterministic model with the $F_{\frac{5}{2}}(\lambda)$ function calculated from the generated probability functions using the Greenwood and Tripp approach is shown in **Figure 2** along with the load carrying capacity predicted by a curve fit of the $F_{\frac{5}{2}}(\lambda)$ function provided by Arcoumanis (1997) for a Gaussian peak height distribution.

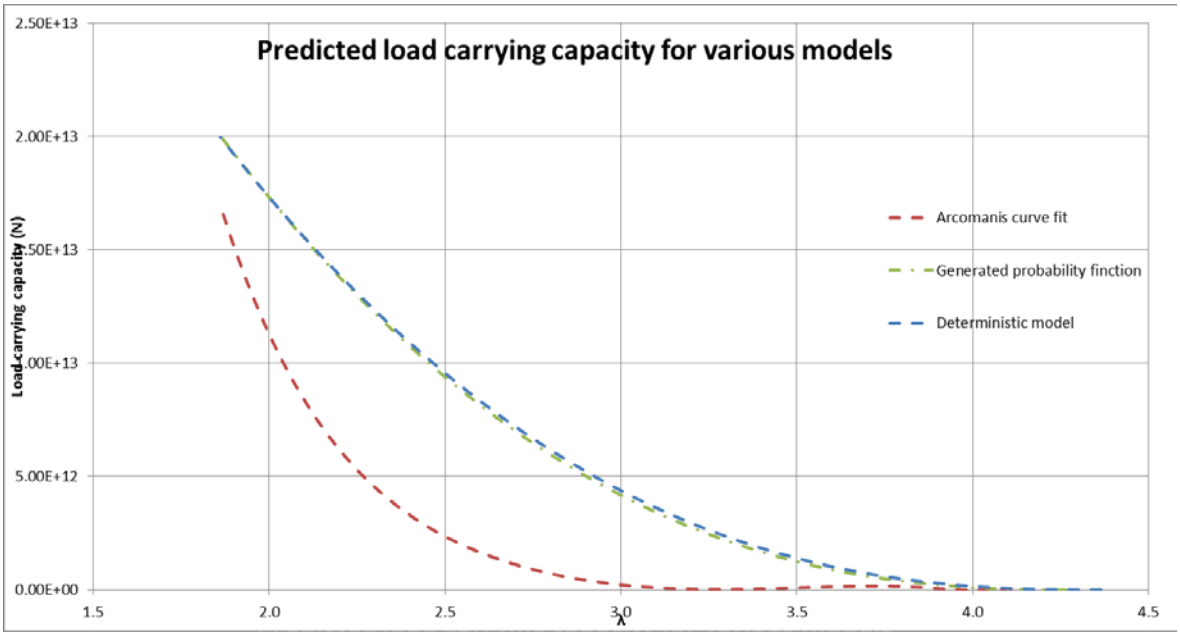

Figure 2 Predicted Load carrying capacity for various models

It can be seen from the comparison that there is very strong agreement between the deterministic model and the Greenwood and Tripp approach using the surface data specific to this case, validating the program used.

5. RESULTS FOR MEASURED SURFACES

Surface data from real measure surfaces were then used in order to determine a more realistic $F_{\frac{5}{2}}(\lambda)$ function. The surfaces considered were those of (surface 1) a flat plate with a skewed surface height distribution and surface finish similar to that seen on a honed cylinder liner and (surface 2) a corresponding flat surface with an approximately Gaussian surface height distribution and low RMS roughness similar to that of a piston ring. The peak height distributions of these surfaces and the convoluted peak height distribution can be seen below (**Figure 3-5**). Since the peak height distributions taken are for dissimilar surfaces the peak height distributions must be adjusted individually before they are combined in the convolution. The total area under the distributions for each surface is set to unity and the centre point of the distribution (λ=0) is set at the mean surface height position.

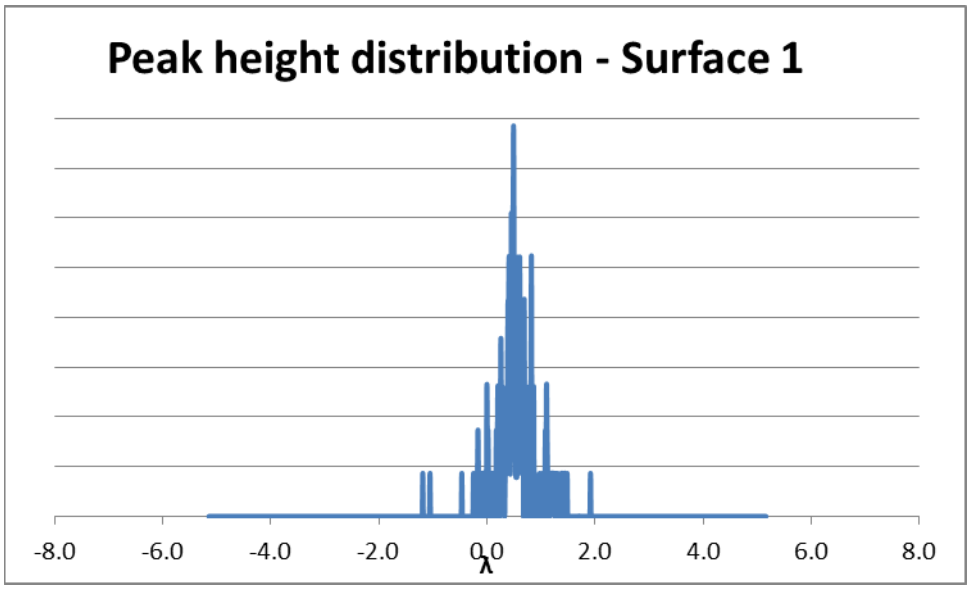

Figure 3 Peak height distribution for surface 1

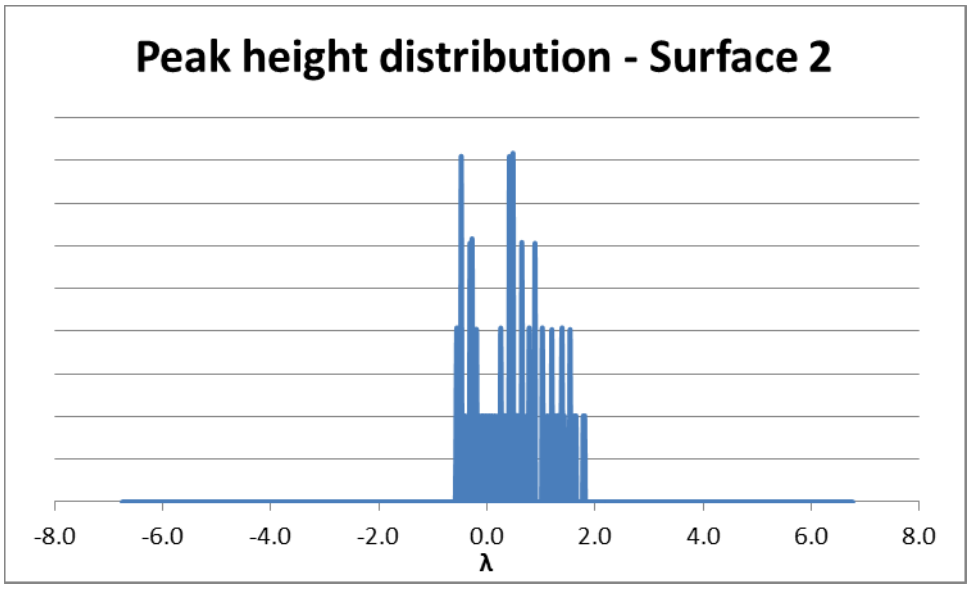

Figure 4 Peak height distribution for surface 2

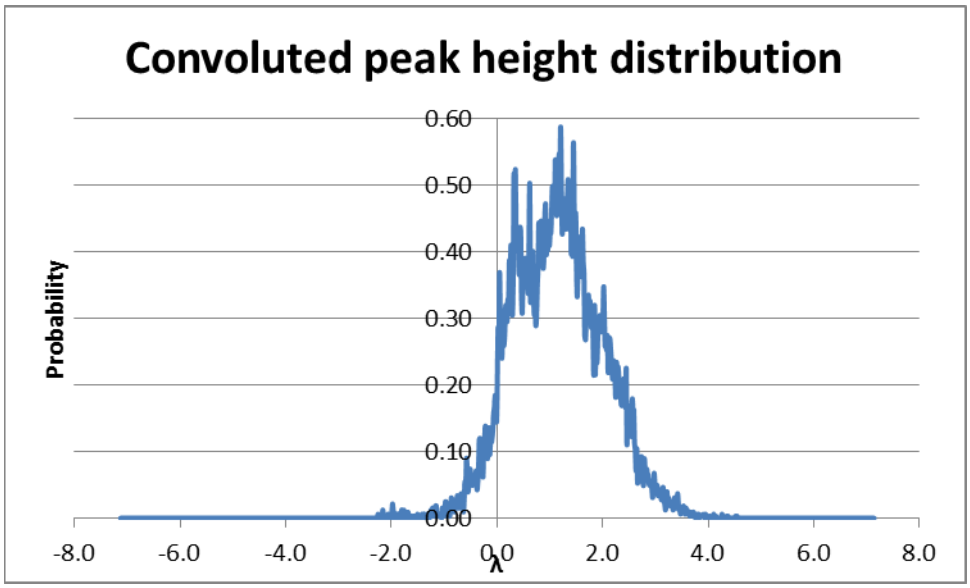

Figure 5 Convoluted peak height distribution

Finally a comparison between the surface specific $F_{\frac{5}{2}}(\lambda)$ function and the $F_{\frac{5}{2}}(\lambda)$ function provided by Greenwood and Tripp for a Gaussian surface distribution, to which Arcoumanis fitted a 6th order curve fit is given (**Figure 6**)

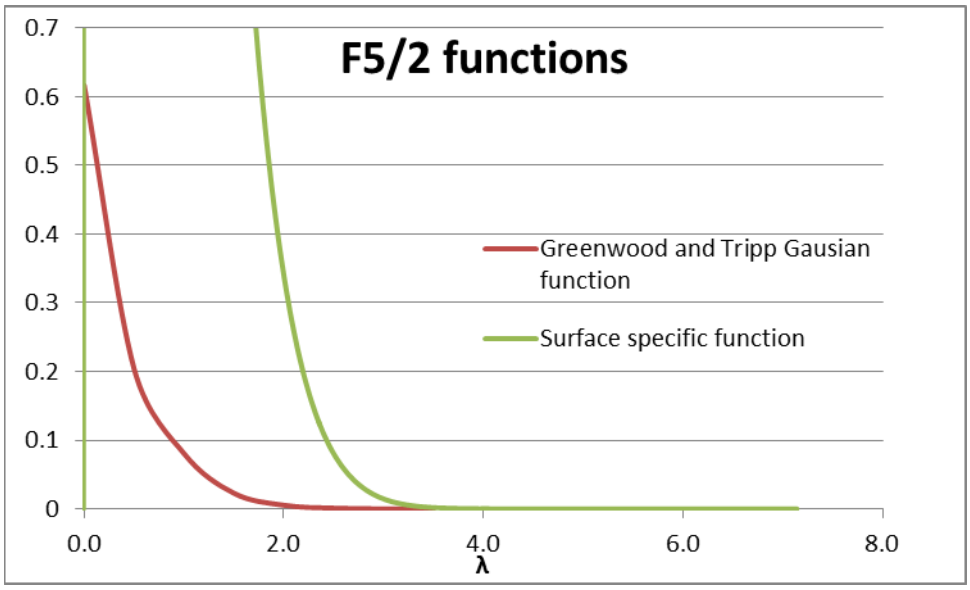

Figure 6 F5/2 function

6. CONCLUSIONS

It can be seen from **Figure 6** that there is significant difference in the functions and the surface specific function climbs much more steeply than the Gaussian function. This is due in part to the increased proportion of asperities in the higher regions of the surface. There is therefore a greater cumulative effect of these and as the surface is lowered those asperities continue to compress by increasing amounts. It can be seen from the convolution of the peak height distributions (**Figure 5**) that there are significantly more asperities above the centreline of the surface than below as might be expected. This not only produces a non-Gaussian peak distribution but the mean is non-zero which should also be seen in the surface with a Gaussian peak height distribution but was not accounted for in the curve fit provided by Greenwood and Tripp.

It is clear that using a $F_{\frac{5}{2}}(\lambda)$ function generated from real surface data will produce a significant difference in the predicted load carrying capacity of a surface at a given separation and real surface data should be used for modelling wherever higher precision of predictions is required.

ACKNOWLEDGEMENTS

The authors would like to thank Capricorn Automotive for their cooperation and support in this project.

REFERENCES

Arcoumanis, C, Ostovar, P, Mortier, R. Mixed lubrication modelling of Newtonian and shear thinning liquids in a piston-ring configuration. SAE Technical Paper Series 1997; 972924:35 (Reference to a journal publication)

Greenwood, J, Tripp, J. Contact of two nominally flat rough surfaces. Proc. IMechE 1970; 185:625 (Reference to a journal publication)

Greenwood, J, Williamson, J. Contact of nominally flat surfaces. Proc. R. Soc. Lond. A 1966; 295 (Reference to a journal publication)

Mishra, P, Rahnejat, H, King, P. Tribology of the ring–bore conjunction subject to a mixed regime of lubrication. Proc. IMechE Part C: Journal of Mechanical Engineering Science 2009; 223:987 (Reference to a journal publication)

Morris, N, Rahmani, R, Rahnejat, H, King, P, Fitzsimons, B. Tribology of piston compression ring conjunction under transient thermal mixed regime of lubrication. Tribology International 2013; 59:248–258 (Reference to a journal publication)

Peklenik, J. New developments in surface characterization and measurements by means of random process analysis. Proc. IMechE Conference Proceedings 1967; 182:108 (Reference to a journal publication)

Rahmani, R, Theodossiades S, Rahnejat, H, Fitzsimons, B. Transient elastohydrodynamic lubrication of rough new or worn piston compression ring conjunction with an out-of-round cyliner bore. Proc. IMechE Part J: Engineering Tribology 2012; 226(4):284–305 (Reference to a journal publication)